Supplementary Information (SI) for ChemComm.
This journal is © The Royal Society of Chemistry 2026

Supporting Information

Redox-Active Multi-Thianthrene Cycloparaphenylenes: Synthesis and Supramolecular Properties

*Tara D. Clayton, Veronica R. Spaulding, Audrey M. Davenport, Lev. N. Zakharov, Carl K. Brozek, Ramesh Jasti**

Table of Contents

1. Experimental details

Unless otherwise noted, commercially available materials were used without purification. Compounds **3** and **4** were prepared according to the literature.[1–3] Moisture and oxygen sensitive reactions were carried out in flame-dried glassware and under an inert atmosphere of purified nitrogen using syringe/septa technique. Tetrahydrofuran (THF) and dimethylformamide (DMF) were dried by filtration through alumina according to the methods described by Grubbs.[4] Alumina column chromatography was conducted with SorbTech basic alumina (pH 10), Act. II-III, 50-200 µm. ^{1}H and ^{13}C NMR spectra were recorded on a Bruker Avance III HD 500 (^{1}H: 500 MHz, ^{13}C: 126 MHz) NMR spectrometer. The chemical shifts (δ) were reported in parts per million (ppm) and were referenced to the residual protio-solvent (CD_2Cl_2, ^{1}H: δ = 5.32 ppm and ^{13}C: δ = 53.84 ppm; deuterated 1,1,2,2-tetrachloroethane (TCE-d_2), ^{1}H: δ = 6.00 ppm and 13C: δ = 73.78 ppm) or to tetramethylsilane (for $CDCl_3$, TMS, δ = 0.00 ppm). Coupling constants (J) are given in Hz and the apparent resonance multiplicity is reported as s (singlet), d (doublet), t (triplet), q (quartet), dd (doublet of doublets) or m (multiplet). UV/Vis absorption and fluorescence spectra were recorded on an Agilant Cary 100 spectrophotometer and a Horiba Jobin Yvon Fluoromax-4 Fluorimeter, respectively. All measurements were carried out under ambient conditions in a Spectrocell RF-1010-T threaded top vacuum formed borosilicate fluorometer cell (10 mm light path). Supplementary raw data files including BindFit data are available *via* Figshare: https://figshare.com/account/articles/31259227.

2. Synthesis

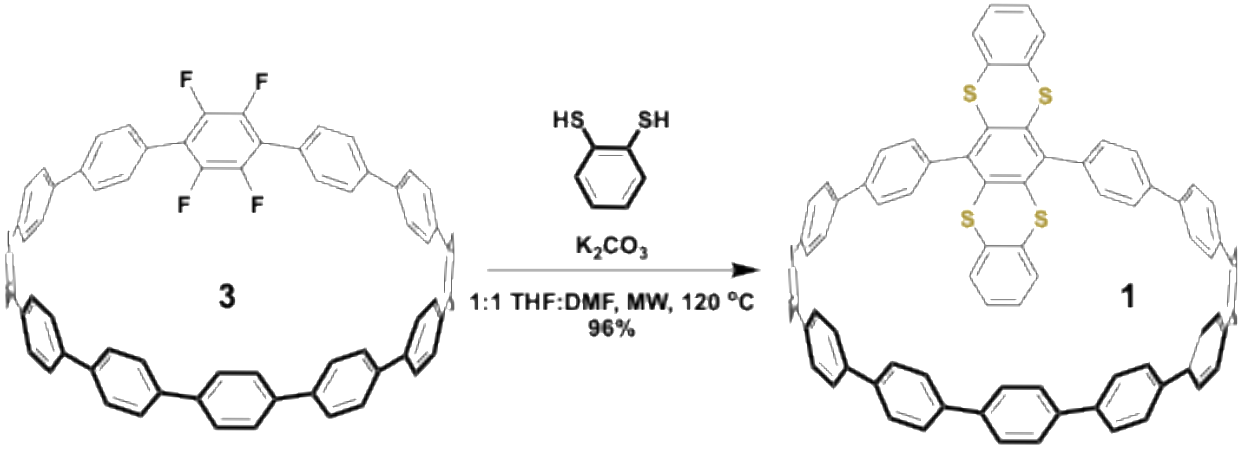

Compound 1: 3 (16.4 mg, 0.017 mmol, 1 eq), 1,2-Benzenedithiol (0.019 mL, 0.166 mmol, 10 eq), and K_2CO_3 (13.8 mg, 0.01 mmol, 6 eq) were added to a microwave flask and dissolved in THF (0.55 mL, 0.03 M) and DMF (0.55 mL, 0.03 M). The reaction mixture was heated with microwave to 120 °C and allowed stir for 24 hrs. It was then cooled to room temperature and diluted with DCM and water. A 1M aqueous solution of K_2CO_3 was added until the solution was basic, and the product was extracted with DCM (4 X 50 mL), washed with water (2 X 50 mL), washed with brine (2 X 50 mL), dried over sodium sulfate, filtered, and concentrated. Finally, the material was rinsed with methanol and dried to afford the product as an off-white powder (19 mg) in 96% yield. ^{1}H NMR (500 MHz, Methylene Chloride-d_2) δ 7.77 – 7.63 (m, 40H), 7.26 (d, *J* = 8.2 Hz, 4H), 7.06 (dd, *J* = 5.8, 3.4 Hz, 4H), 6.95 (dd, *J* = 5.8, 3.4 Hz, 4H). ^{13}C NMR (126 MHz, CD_2Cl_2) δ 141.05, 140.05,

139.23, 138.59, 138.56, 138.54, 138.52, 138.49, 138.45, 138.38, 137.49, 135.79, 135.54, 130.99, 128.36, 127.98, 127.60, 127.42, 127.36, 127.34, 127.29, 127.27, 127.12. HRMS (MALDI) m/z: [M]+ calculated for $C_{84}H_{52}S_4$ 1188.2952, found 1188.2967.

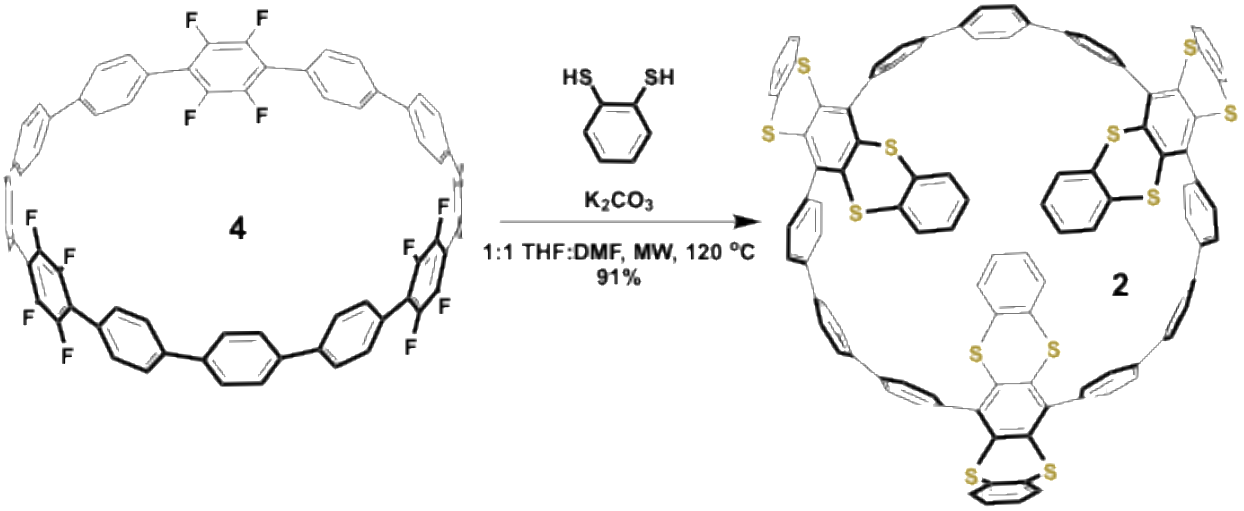

Compound 2: 4 (9.3 mg, 0.008 mmol, 1 eq), 1,2-Benzenedithiol (0.008 mL, 0.066 mmol, 8 eq), and K_2CO_3 (20 mg, 0.148 mmol, 18 eq) were added to a microwave flask and dissolved in THF (0.55 mL, 0.015 M) and DMF (0.55 mL, 0.015 M). The reaction mixture was heated with microwave to 120 °C and allowed stir for 24 hrs. It was then cooled to room temperature and diluted with DCM and water. A 1M aqueous solution of K_2CO_3 was added until the solution was basic, and the product was extracted with DCM (4 X 50 mL), washed with water (2 X 50 mL), washed with brine (2 X 50 mL), dried over sodium sulfate, filtered, and adsorbed onto basic alumina. An alumina plug eluted with DCM in hexanes (0-100%) afforded the product as an off-white powder (13 mg) in 91% yield. ^{1}H NMR (500 MHz, Methylene Chloride-d_2) δ 7.78 – 7.57 (m, 24H), 7.53 (s, 4H), 7.41 (dd, *J* = 21.4, 7.3 Hz, 6H), 7.29 (dd, *J* = 25.7, 8.2 Hz, 12H), 7.16 (dd, *J* = 5.7, 3.4 Hz, 2H), 7.13 – 7.06 (m, 6H), 6.97 (dd, *J* = 13.2, 5.7 Hz, 6H). ^{13}C NMR (126 MHz, CD_2Cl_2) δ 141.01, 140.11, 139.66, 136.40, 135.93, 135.83, 135.75, 135.64, 131.74, 131.48, 129.13, 128.67, 128.49, 128.30, 127.79, 127.22, 127.06, 126.88. HRMS (MALDI) m/z: [M]+ calculated for $C_{108}H_{60}S_{12}$ 1740.1344, found 1740.1354.

3. Nuclear magnetic resonance spectra

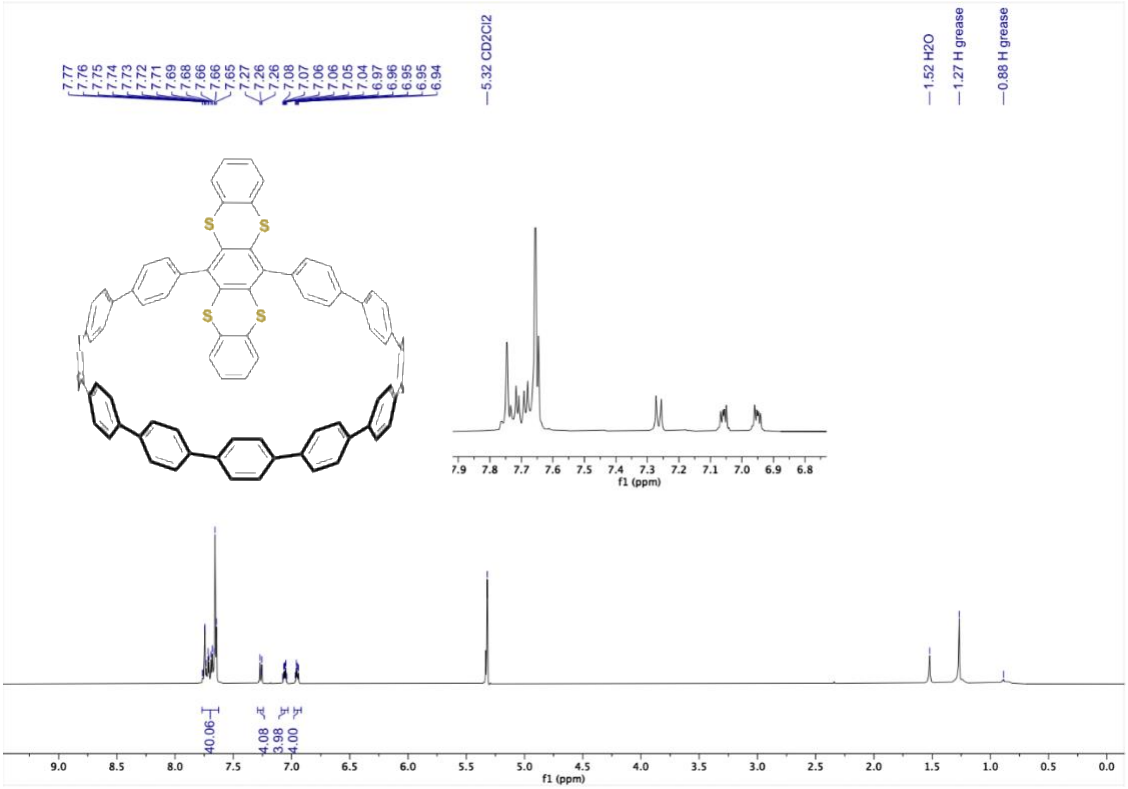

Figure S1. ^{1}H NMR Spectrum of **1.**

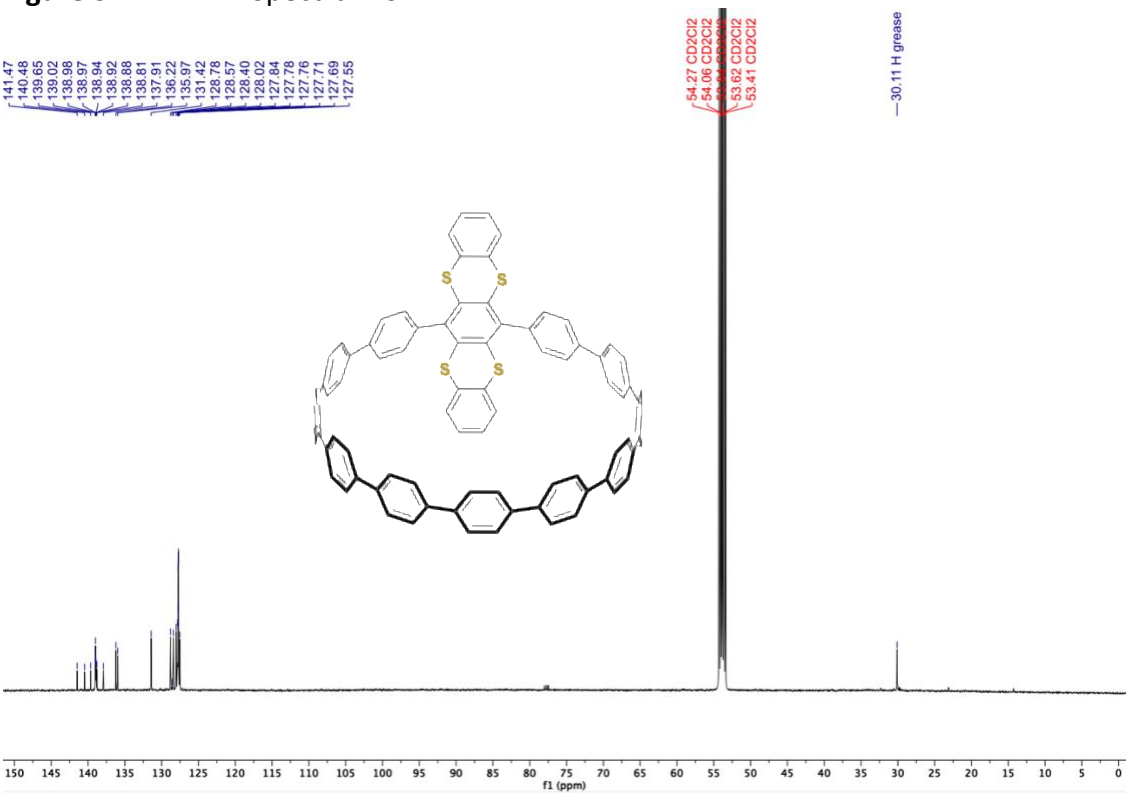

Figure S2. ^{13}C NMR Spectrum of **1.**

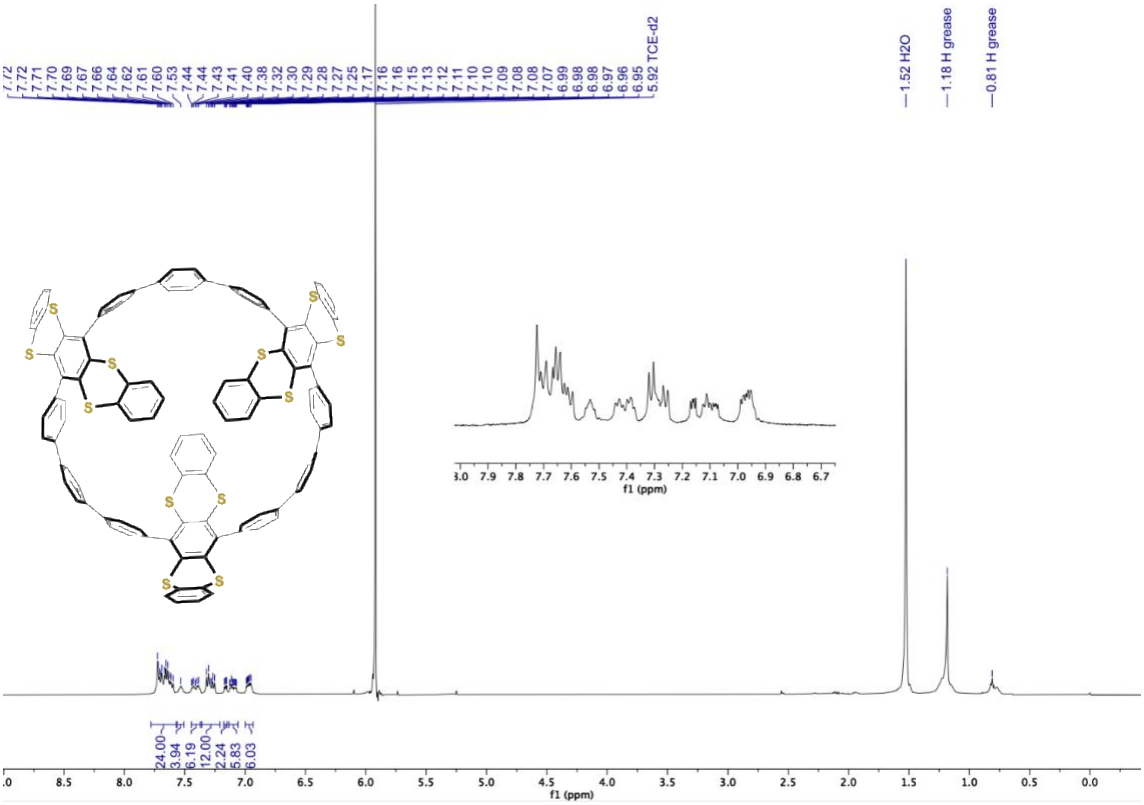

Figure S3. ^{1}H NMR Spectrum of **2.** The reactions were run on a small scale, and despite not detecting any other byproducts, we were unable to isolate **2** without grease contamination.

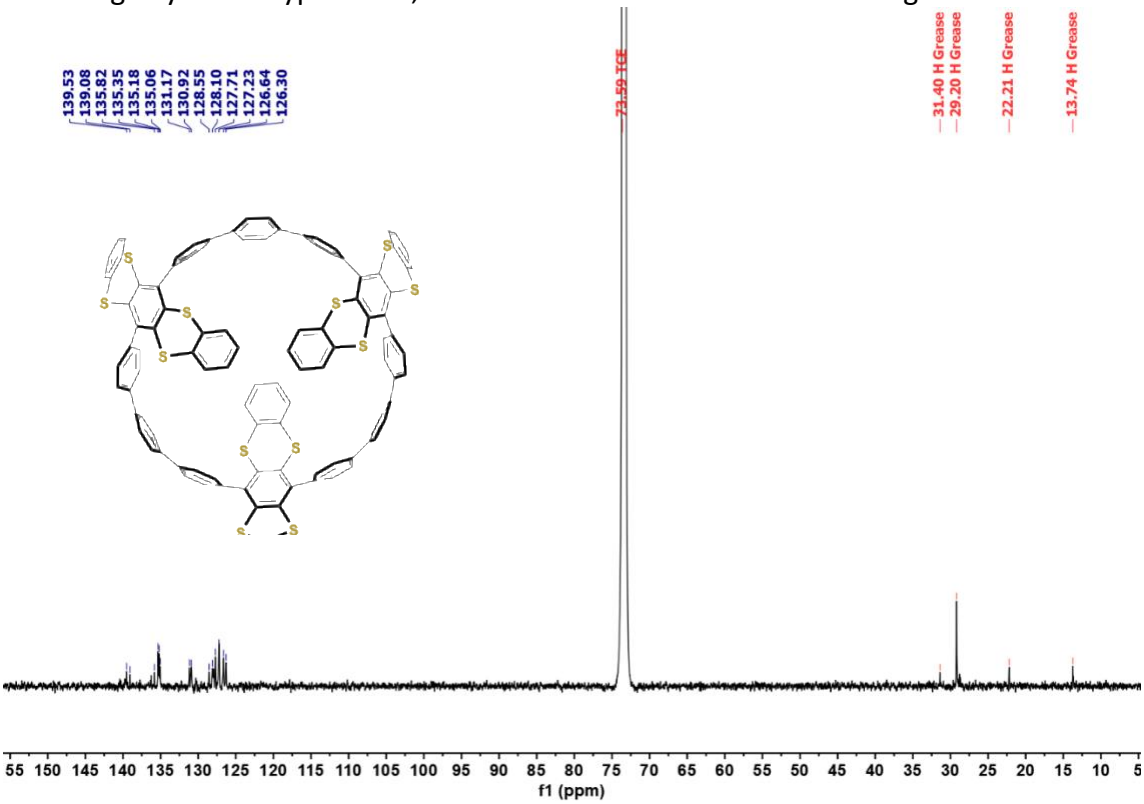

Figure S4. ^{13}C NMR Spectrum of **2.**

4. High-resolution mass spectra

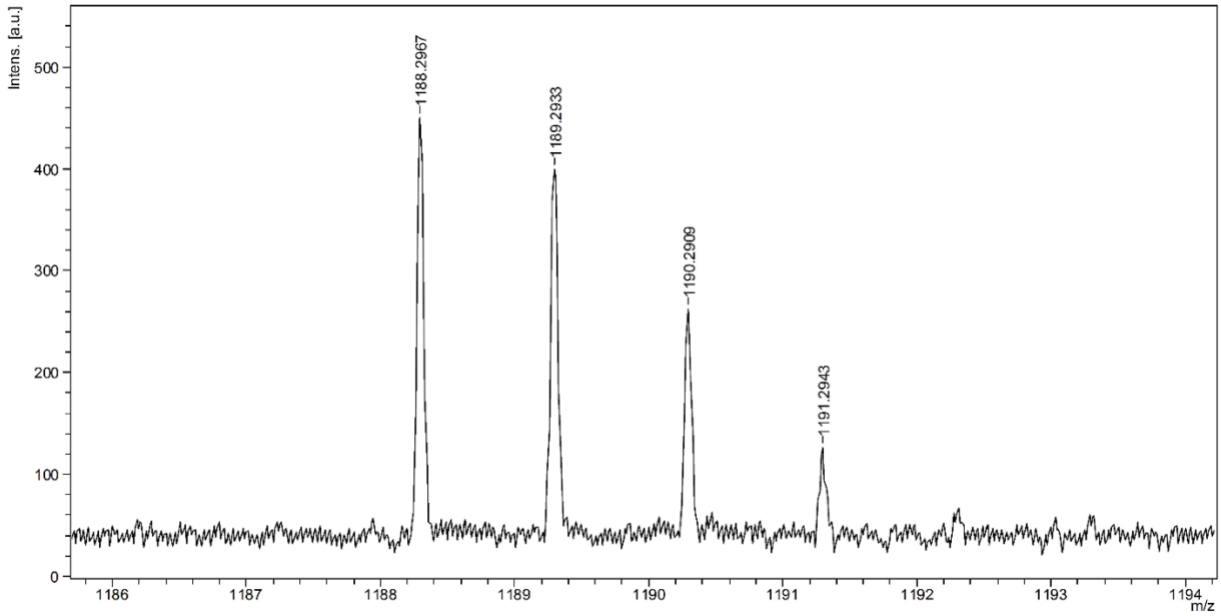

Figure S5. High-resolution MALDI-TOF mass spectrum of **1.**

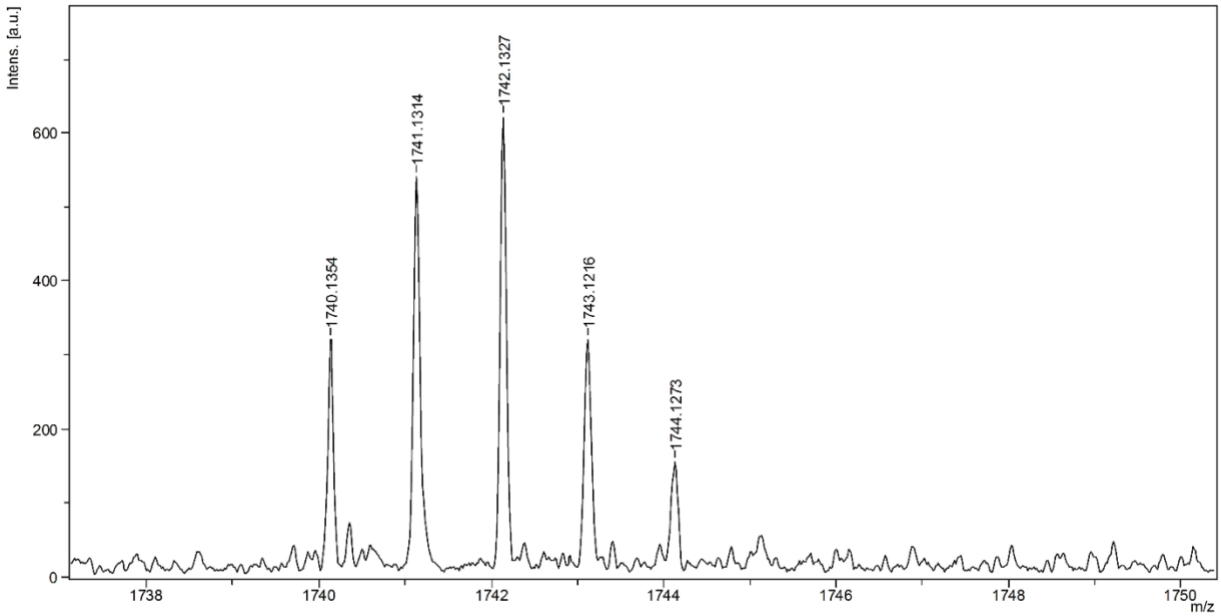

Figure S6. High-resolution MALDI-TOF mass spectrum of **2.**

5. X-ray crystallographic information

X-ray Crystallography. Diffraction intensities for **2** were collected at 173 K on a Bruker Apex2 single crystal diffractometer using CuKα radiation, 1.54178 Å. Space group was determined based

on systematic absences. Absorption correction was applied by SADABS[*]. Structure was solved by direct methods and Fourier techniques and refined on F^2 using full matrix least-squares procedures. All non-H atoms were refined with anisotropic thermal parameters. H atoms in the structure were refined in calculated positions in a rigid group model. The diffraction data at high angles are very weak due to a strong disorder of solvent molecules. They were collected only up to resolution 1.01 Å even by using a strong *Incoatec* Cu-source. However, it provides the appropriate ratio of the number of the measured reflections per the number of the refined parameters, 12202/1142. Two $CHCl_3$ solvent molecules located outside the hoop were found from the XRD data and refined. Others solvent molecules located inside the hoop are highly disordered and were treated by SQUEEZE[**]. Solvent molecules treated by SQUEEZE were not included in the total formula of the compound given in the CIF file. The structure was determined in a non-centrosymmetrical space group as a racemic twin: the Flack is 0.12(3). One of the $S_2C_6H_4$ groups is highly disordered. Atomic thermal parameters in this group are elongated, and this group was refined as a C6-group with the ideal geometry. The RIGU option was used in the structure refinement. The structure is determined with a low resolution. However, the X-ray structure provides the clear chemical results. All calculations were performed by the Bruker SHELXL-2014/7 package [***].

Crystallographic Data for Jastirr212: $C_{110}H_{62}Cl_6S_{12}$, M = 1981.01, 0.15 x 0.14 x 0.08 mm, T = 173(2) K, Hexagonal, space group $P6_5$, a = 19.6392(4) Å, b = 19.6392(4) Å, c = 53.6698(19) Å, α = 90°, β = 90°, γ = 120.0°, V = 17927.0(10) Å^3, Z = 6, Dc = 1.101 Mg/m^3, μ(Cu) = 3.582 mm^{-1}, F(000) = 6096, $2\vartheta_{max}$ = 100.134°, 87596 reflections, 12202 independent reflections [R_{int} = 0.1647], R1 = 0.0717, wR2 = 0.1832 and GOF = 1.028 for 12202 reflections (1142 parameters) with I>2σ(I), R1 = 0.1057, wR2 = 0.2059 and GOF = 1.001 for all reflections, the Flack = 0.12(3), max/min residual electron density +0.268/-0.293 eÅ^{-3}.

5. Photophysical Characterization

6 a. UV-Vis and Fluorescence

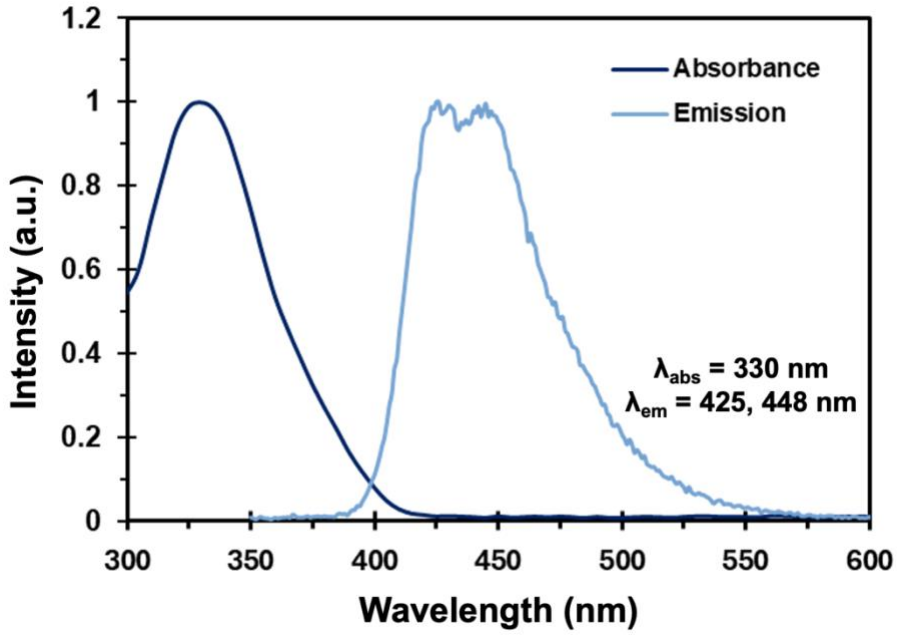

Figure S7. Normalized absorbance (dark blue) and fluorescence (light blue) of **1** in dichloromethane with λ_{max} at 330 nm and λ_{em} at 425, 448 nm.

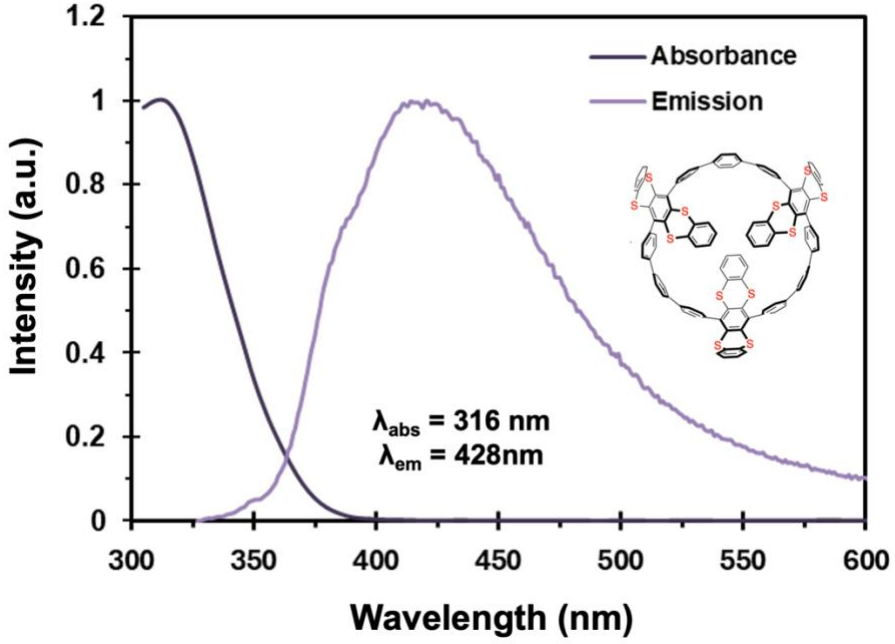

Figure S8. Normalized absorbance (dark purple) and fluorescence (light purple) of **2** in dichloromethane with λ_{max} at 316 nm and λ_{em} at 428 nm.

6 b. Solvatochromism Study of 2

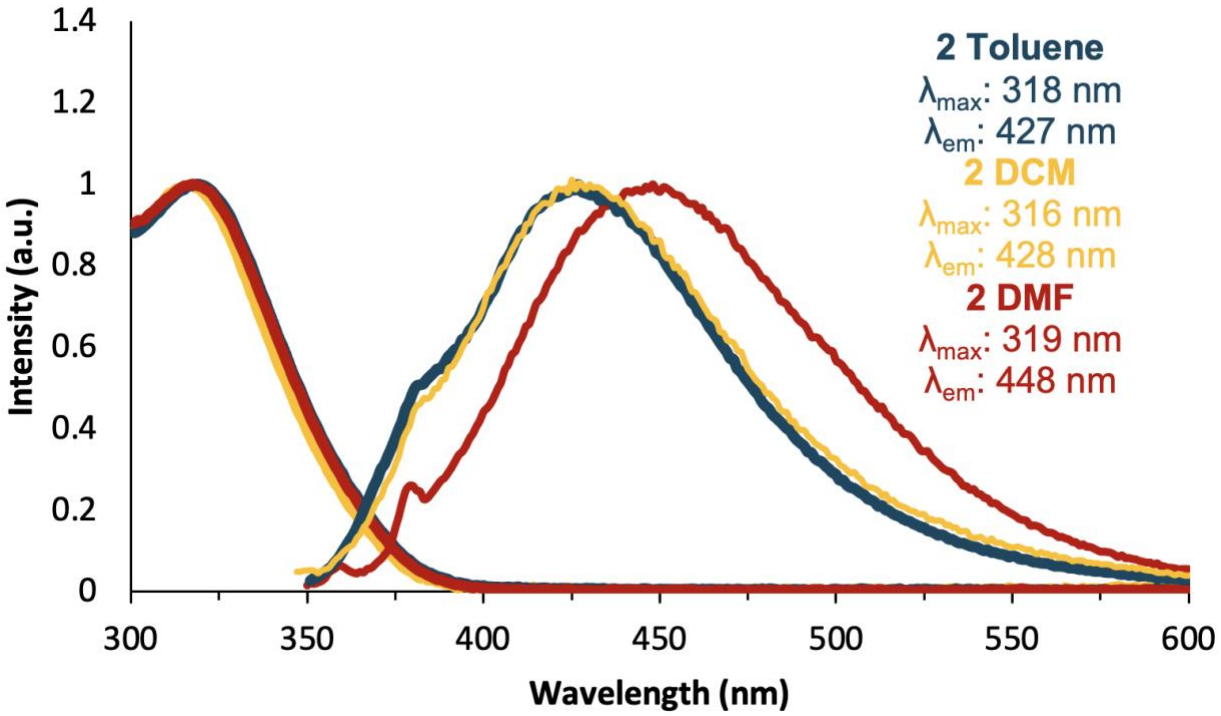

Figure S9. Normalized absorbance and fluorescence of **2** in various solvents excited at 340 nm.

6 c. Extinction Coefficient Measurements

For extinction coefficient measurements, **1** and **2** were dissolved at known concentrations in dichloromethane. Solutions of **1** and **2** were then added incrementally to a cuvette containing a known amount of dichloromethane and absorbance measurements were taken after each addition. The whole process was repeated three times for **1** and **2** respectively. Data was worked up by dividing the absorbance value at the absorbance maxima by the solution's concentration. Measurements from each trial were averaged together, and the standard deviation between trials was determined.

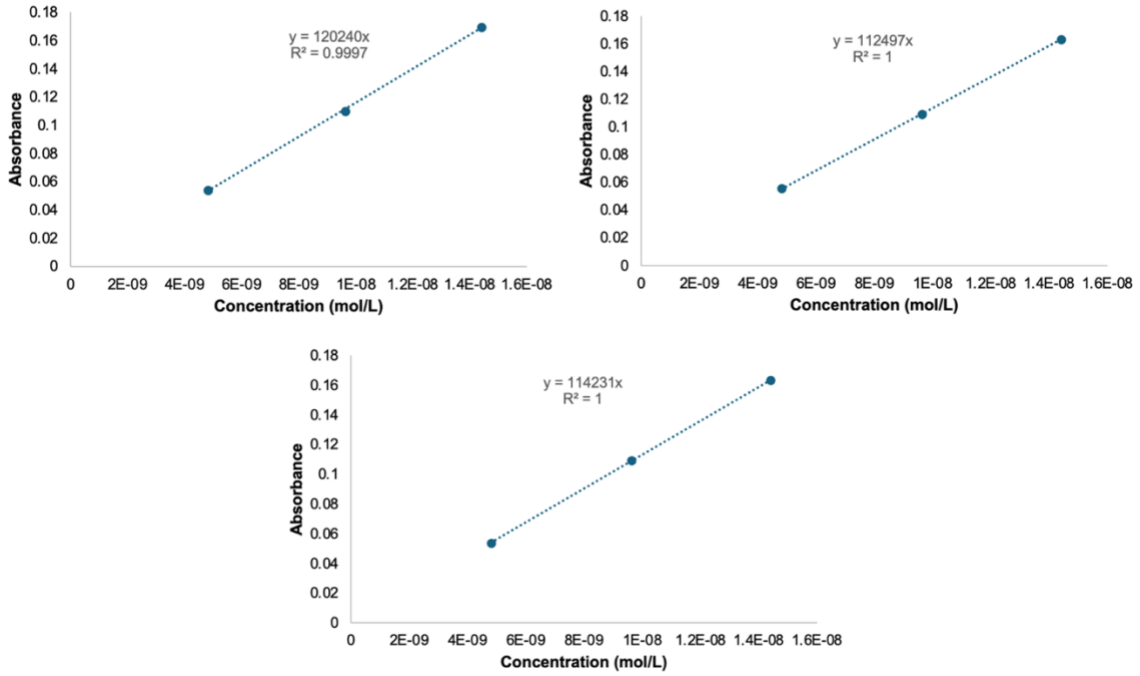

Figure S10. Absorbance versus concentration for extinction coefficient determination of **1** in DCM at the absorbance maximum.

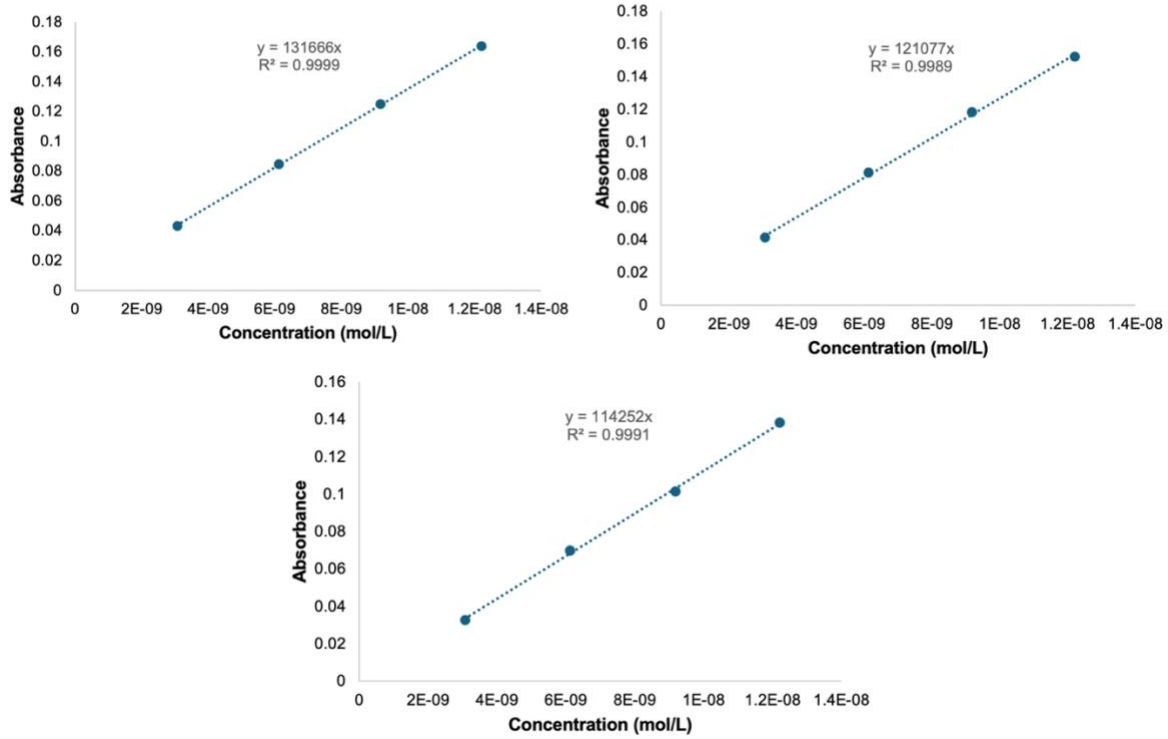

Figure S11. Absorbance versus concentration for extinction coefficient determination of **2** in DCM at the absorbance maximum.

6 d. Quantum Yield Measurements

Quantum yield measurements were performed according to literature procedures.[5,6] Anthracene and quinine were used as standards and found to be within *10%* error from their literature values following established procedures. Parent CPPs (**1p** and **2p**) and Compounds **1** and **2** were all run in CH_2Cl_2. Given the donor-acceptor nature of the thianthrene modified compounds, we see an expected decrease in the QY values. QY values were calculated according to this equation:

$$\varphi_x = \varphi_{ST}\left(\frac{Grad_x}{Grad_{ST}}\right)\left(\frac{\eta_x^2}{\eta_{ST}^2}\right)$$

Where ST = standard and x = test solution, Φ is the fluorescent quantum yield, Grad is the gradient from the plot of the integrated fluorescence intensity vs absorbance, and η is the refractive index of the solvent.

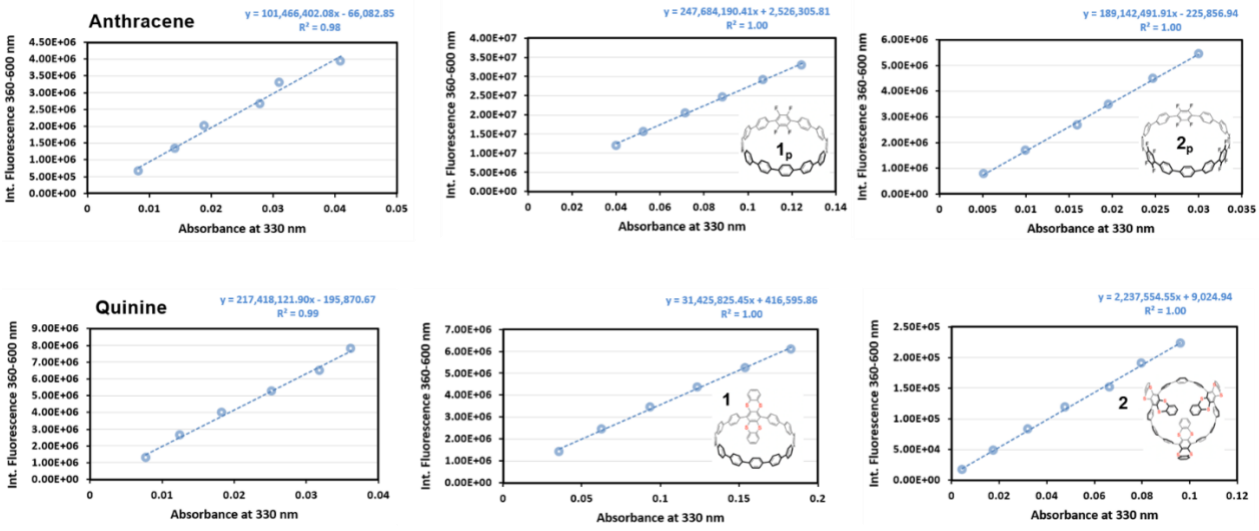

	Lit Val.	n	n²	Slope	Slope Div	n² Div	QY	% error
Quinine	0.54	1.33	1.78	2.17E+08	2.1E+00	9.6E-01	0.55	2.6
Anthracene	0.27	1.36	1.85	1.01E+08	4.7E-01	1.0E+00	0.26	-2.7
1p	w.r.tq	1.42	2.03	2.48E+08	1.1E+00	1.1E+00	0.70	
1p	w.r.ta	1.42	2.03	2.48E+08	2.4E+00	1.1E+00	0.72	
1	w.r.tq	1.42	2.03	3.14E+07	1.4E-01	1.1E+00	0.09	
1	w.r.ta	1.42	2.03	3.14E+07	3.1E-01	1.1E+00	0.09	
2p	w.r.tq	1.42	2.03	1.89E+08	8.7E-01	1.1E+00	0.54	
2p	w.r.ta	1.42	2.03	1.89E+08	1.9E+00	1.1E+00	0.55	
2	w.r.tq	1.42	2.03	2.24E+06	1.0E-02	1.1E+00	0.01	
2	w.r.ta	1.42	2.03	2.24E+06	2.2E-02	1.1E+00	0.01	

Figure S12. Gradients of integrated fluorescent in DCM for quantum yield determination of compounds **1** and **2** (Φ = 1% and 9% respectively).

7. C_{60} Binding Studies

Fluorescence titration experiments were used to determine the association constant (K) between the CPP host (H) **1** and **2** and C_{60} guest (G). Stock solutions of **1**, **2**, and C_{60} were made in toluene at room temperature. Varying concentrations of the C_{60} solution were added to a known concentration of the CPP solution until fluorescence was quenched. All samples were excited at 340 nm. Emission spectra were collected from 345 nm - 800 nm and the fluorescence signal was measured at 426 nm, 448 nm, and 474 nm for **1** and 381 nm, 429 nm, and 450 nm for **2**. Open-source software BindFit was used to fit the data with the Nelder-Mead method.[7]
The association constants were derived by applying a non-linear 1:1 and 2:1 binding model.

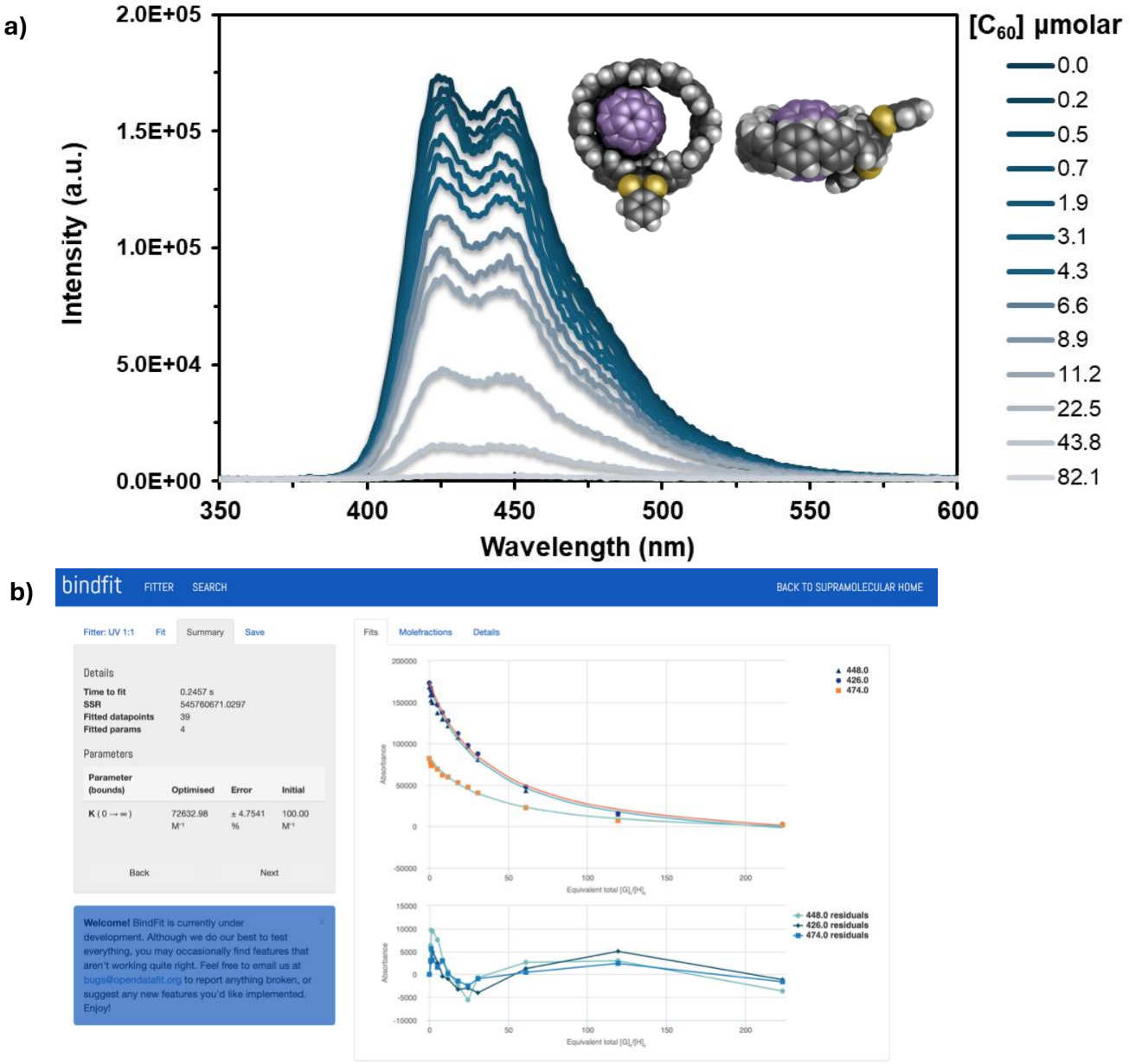

Figure S13. (a) Fluorescence quenching experiment of **1** with increasing amounts of C_{60} guest. (b) Bindfit model demonstrating 1:1 host-guest complexation and binding K_a= 7.26x10^4 M^{-1}.

a)

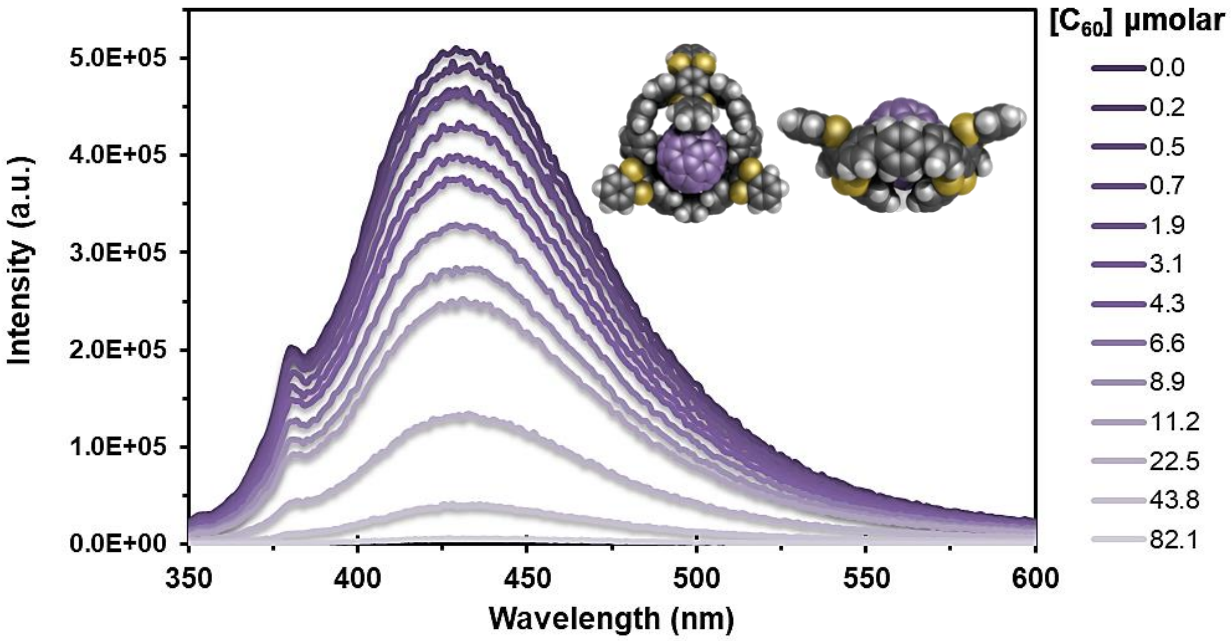

b)

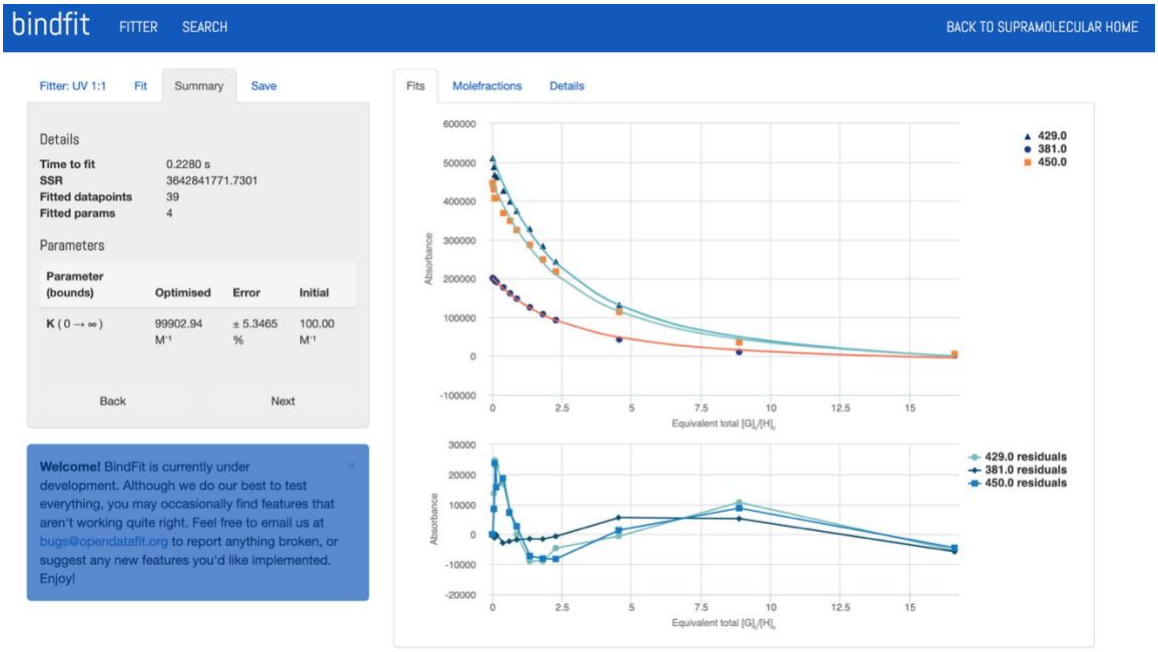

Figure S14. (a) Fluorescence quenching experiment of **2** with increasing amounts of C_{60} guest. (b) Bindfit model demonstrating 1:1 host-guest complexation and binding K_a= 9.99x10^4 M^{-1}.

8. Electrochemical Details

Solutions of **1** and **2** were solubilized separately with $TBAPF_6$ in 1:4 mixtures of acetonitrile:dichlorobenzene to afford 2mM and 0.7mM of the compounds, respectively. Cyclic voltammetry scans were collected at a scan rate of 50mV/s. A graphitic counter electrode and a Ag/Ag^+ pseudo reference electrode were used. Data was all referenced to the Fc/Fc^+ redox couple

in the same solvent mixture. Mixtures were sparged with N_2 for 5 minutes prior to data collection.

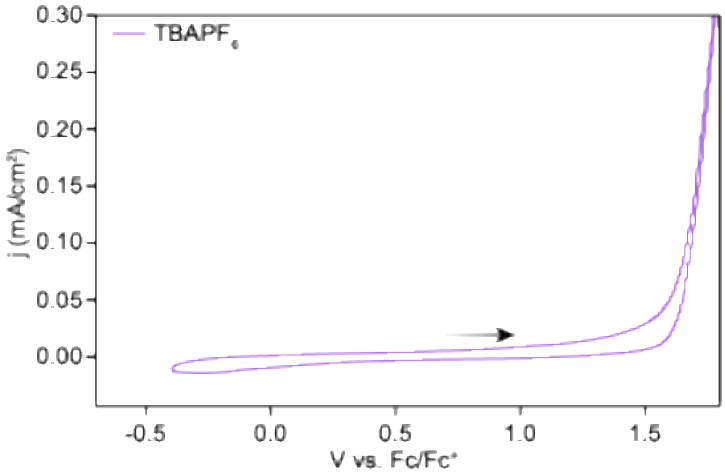

Figure S15: Cyclic voltammetry scan of $TBAPF_6$ in 1:4 mixture of acetonitrile:dichlorobenzene without compounds **1** and **2**. Referenced to the Fc/Fc_+ redox couple.

9. Computational Details

Computational Methods:
Gaussian 09[8] was used for structural geometry minimization, optical vertical transitions, and frequency calculations. All input files are available for download via Figshare at **https://figshare.com/account/articles/31259227?file=61649173.**

Keywords –
a) Geometry Optimization
#n B3LYP/6-31G (d,p) Opt Freq
b) Vertical Transitions
#n B3LYP/6-31G(d,p) TD=NSTATES=12 scrf=(solvent=dichloromethane)
#n CAM-B3LYP/6-31G(d,p) Opt TD scrf=(solvent=dichloromethane)

Vertical transitions were determined using the time-dependent DFT method to probe excited states when exposed to an external field. Optical absorption spectra were observed for 12 states, and emission spectra were found by optimizing the time-dependent excited states. A polarizable continuum model (PCM) was used to better match experimental solvent conditions ran in dichloromethane. Major transitions include degenerate HOMO orbitals to LUMO unoccupied states; similar to parent CPP systems.[9] However, substitution introduces orbital localization on the TTP unit stabilizing occupied orbitals and leads to a hypsochromic shifts the typical CPP 340 nm absorption.

Compound 1 No.	Energy (cm-1)	Wavelength (nm)	Osc. Strength	Symmetry	Major Contributions
1	26474.34258	377.7242049	0.3397	Singlet-A	H-1->L+1 (12%), HOMO->LUMO (83%)
2	28127.77916	355.520425	2.3988	Singlet-A	H-1->LUMO (44%), HOMO->L+1 (48%)
3	29592.482	337.9236659	0.0078	Singlet-A	H-1->LUMO (51%), HOMO->L+1 (45%)
4	29978.82157	333.5688154	0.8715	Singlet-A	H-1->L+1 (62%), HOMO->L+2 (13%)
5	30803.1202	324.6424367	0.5565	Singlet-A	H-1->L+1 (16%), HOMO->L+2 (64%)
6	30954.75243	323.0521718	0.0147	Singlet-A	H-3->LUMO (44%), H-3->L+2 (15%), H-2->LUMO (13%)
7	31198.33187	320.5299579	0.0081	Singlet-A	H-3->L+1 (22%), H-3->L+3 (38%), H-2->L+3 (12%)
8	31294.31185	319.5468892	0.0912	Singlet-A	H-3->LUMO (21%), H-2->LUMO (53%), HOMO->L+2 (16%)
9	31980.68966	312.6886914	0.0063	Singlet-A	H-1->L+2 (13%), HOMO->L+3 (71%)
10	32057.31234	311.9413098	0.0078	Singlet-A	H-1->L+2 (77%)
11	32418.64872	308.46443	0.151	Singlet-A	H-3->L+1 (12%), H-2->L+1 (65%), HOMO->L+3 (11%)
12	32423.48805	308.4183906	0.0006	Singlet-A	H-3->L+1 (52%), H-3->L+3 (21%)

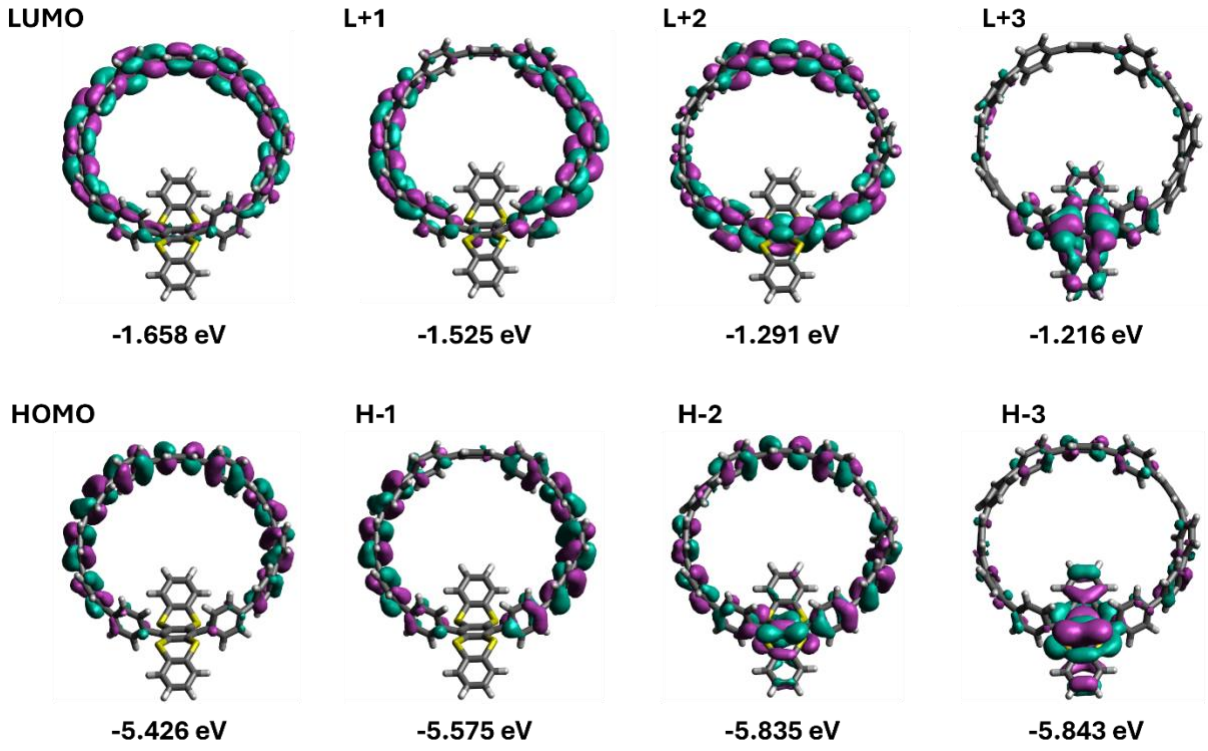

Figure S16. Calculated orbital localization (top) LUMO and (bottom) HOMO for single substitution of tetrathiapentacene on [12]CPP.

No.	Compound 2 Energy (cm-1)	Wavelength (nm)	Osc. Strength	Symmetry	Major Contributions
1	29151.3	343	0.1798	Singlet-A	H-1->LUMO (36%), H-1->L+1 (14%)
2	29296.5	341	0.1835	Singlet-A	H-3->LUMO (27%), H-1->LUMO (12%), HOMO->LUMO (11%)
3	29387.6	340	0.0479	Singlet-A	H-2->LUMO (48%), HOMO->L+1 (13%)
4	30123.2	332	0.8993	Singlet-A	H-2->L+1 (17%), HOMO->LUMO (27%), HOMO->L+2 (18%)
5	30199.8	331	0.1445	Singlet-A	H-3->L+3 (14%), HOMO->L+3 (57%)
6	30453.1	328	0.0035	Singlet-A	H-3->L+5 (24%), H-1->L+5 (47%)
7	30547.4	327	0.0191	Singlet-A	H-3->L+4 (33%), H-1->L+4 (24%)
8	30647.5	326	0.4774	Singlet-A	H-4->LUMO (17%), H-2->L+1 (20%)
9	30832.2	324	0.9958	Singlet-A	H-5->LUMO (25%), H-2->L+2 (19%), HOMO->L+1 (16%)
10	31425.8	318	0.1251	Singlet-A	H-4->L+1 (14%), HOMO->L+1 (39%)
11	31638.7	316	0.0397	Singlet-A	H-3->L+2 (22%), H-1->L+1 (34%), HOMO->L+2 (11%)
12	31725.8	315	0.0205	Singlet-A	H-3->L+1 (17%), H-1->L+2 (33%)

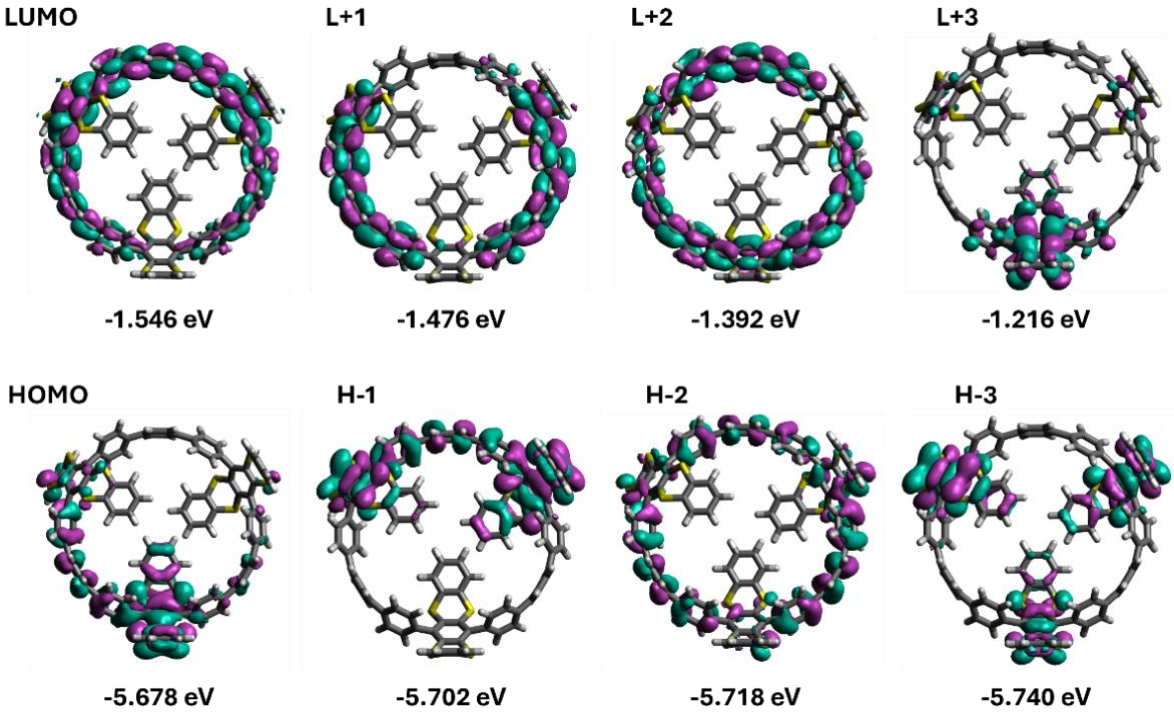

Figure S17. TD-DFT orbital localization for (top) LUMO and (bottom) HOMO for trisubstituted tetrathiapentacene on [12]CPP.

c) Binding Energy

#n M062X/6-31G(d,p) Opt Freq scrf=(solvent=toluene)

Binding energy calculations were performed using G09[8] at the M06-2X level of theory to compare to literature values of cycloparaphenylenes and visualized using PyMOL.[10,11] Frequency calculations were performed with the polarizable continuum model (PCM) to better represent toluene solvation. Binding analysis was performed by computing the difference of the sums of values for the reactants (Host, Guest) and products (Complex) to derive corrected Gibbs free energy values, see equation 1.[12] We see that as we increased the number of thianthrene units we can increase [12]CPPs binding to C60. M06-2X is known to overestimate binding energy, in the case for [10]CPP it is highly overestimated (ΔG°_{lit}=37 kj/mol, ~121% overestimate) perhaps due to closer H contacts as seen in previous literature DFT results.[10,11] However, with substituted [12]CPP variations it better estimates C60 binding compared to experimental observations (~6 to 21% differences -See **Table S1**). Although there is error in the computations, we see the same trend of an increase in host binding upon TTP substitution as observed experimentally.

$$\Delta_r G^{\circ}(298K) = \sum(\mathcal{E}_0 + G_{corr})_{\text{products}} - \sum(\mathcal{E}_0 + G_{corr})_{\text{reactants}} \quad \textbf{(1)}$$

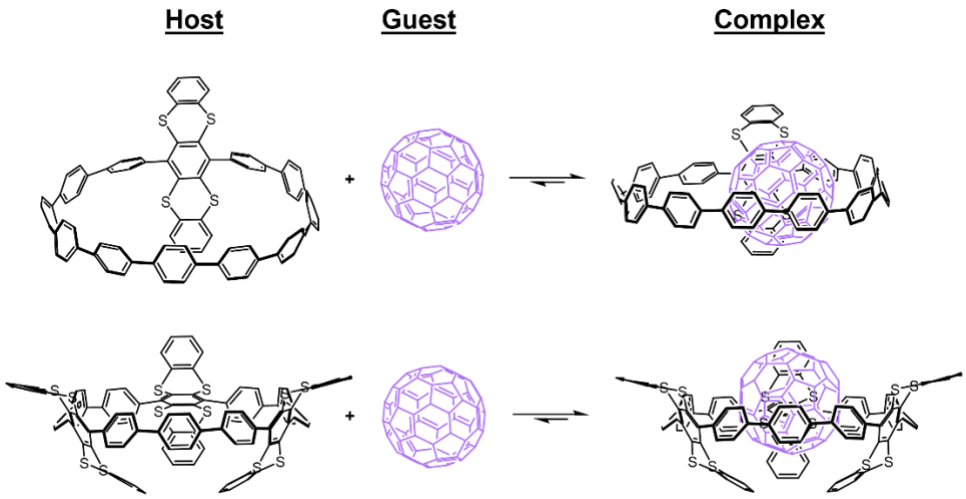

Complex	ΔG Total (kJ/mol)	Error (%)
[10]CPP DFT	-82	
[10]CPP Lit. EXP	-37	-121.6
2 DFT	-31	
2 EXP (1:1)	-29	6.9
1 DFT	-22	
1 EXP (1:1)	-27.7	20.6

Table S1. Free energy comparisons for computed and experimental binding of C_{60} guest complexation.

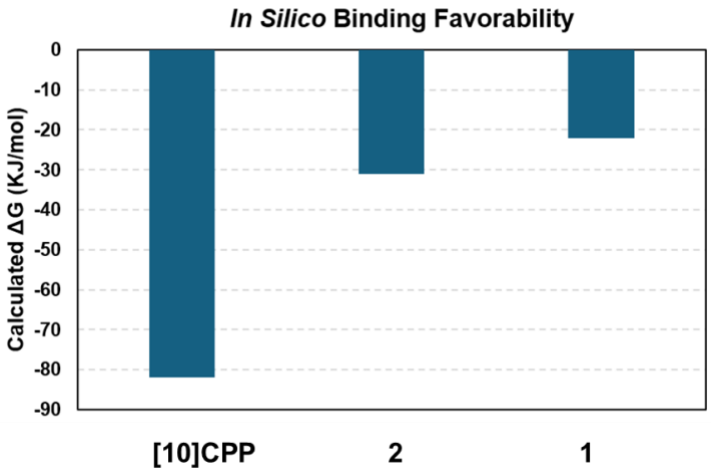

Figure S18. DFT calculated free energy for complex **1**, **2**, and **[10]CPP**. Computed with G09 at the M06-2X level of theory in a toluene solvation model.

DFT Calculated Complexes:

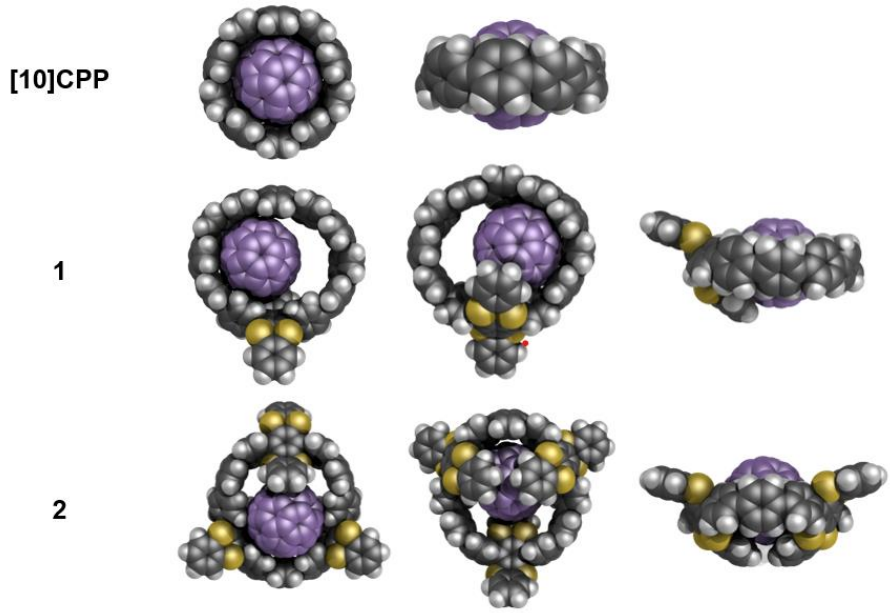

Figure S19. G09 minimized geometry structures of hydrocarbon and TTP-CPPs visualized in PyMOL.

10. References

1 T. A. Schaub, J. T. Margraf, L. Zakharov, K. Reuter and R. Jasti, *Angew. Chem. Int. Ed.*, 2018, **57**, 16348–16353.

2 N. C. Bruno, M. T. Tudge and S. L. Buchwald, *Chem. Sci.*, 2013, **4**, 916–920.

3 J. M. Fehr, N. Myrthil, A. L. Garrison, T. W. Price, S. A. Lopez and R. Jasti, *Chem. Sci.*, 2023, **14**, 2839–2848.

4 A. B. Pangborn, M. A. Giardello, R. H. Grubbs, R. K. Rosen and F. J. Timmers, *Organometallics*, 1996, **15**, 1518–1520.

5 T. D. Clayton, J. M. Fehr, T. W. Price, L. N. Zakharov and R. Jasti, *J. Am. Chem. Soc.*, 2024, **146**, 30607–30614.

6 H. Scientific, .

7 D. B. Hibbert and P. Thordarson, *Chem. Commun.*, 2016, **52**, 12792–12805.

8 M. J. Frisch, G. W. Trucks, H. B. Schlegel, G. E. Scuseria, M. A. Robb, J. R. Cheeseman, G. Scalmani, V. Barone, G. A. Petersson, H. Nakatsuji, X. Li, M. Caricato, A. V. Marenich, J. Bloino, B. G. Janesko, R. Gomperts, B. Mennucci, H. P. Hratchian, J. V. Ortiz, A. F. Izmaylov, J. L. Sonnenberg, Williams, F. Ding, F. Lipparini, F. Egidi, J. Goings, B. Peng, A. Petrone, T. Henderson, D. Ranasinghe, V. G. Zakrzewski, J. Gao, N. Rega, G. Zheng, W. Liang, M. Hada, M. Ehara, K. Toyota, R. Fukuda, J. Hasegawa, M. Ishida, T. Nakajima, Y. Honda, O. Kitao, H. Nakai, T. Vreven, K. Throssell, J. A. Montgomery Jr., J. E. Peralta, F. Ogliaro, M. J. Bearpark, J. J. Heyd, E. N. Brothers, K. N. Kudin, V. N. Staroverov, T. A. Keith, R. Kobayashi, J. Normand, K. Raghavachari, A. P. Rendell, J. C. Burant, S. S. Iyengar, J. Tomasi, M. Cossi, J. M. Millam, M. Klene, C. Adamo, R. Cammi, J. W. Ochterski, R. L. Martin, K. Morokuma, O. Farkas, J. B. Foresman and D. J. Fox, Gaussian 16 Rev. C.01 2016.

9 L. Adamska, I. Nayyar, H. Chen, A. K. Swan, N. Oldani, S. Fernandez-Alberti, M. R. Golder, R. Jasti, S. K. Doorn and S. Tretiak, *Nano Lett.*, 2014, **14**, 6539–6546.

10 T. Iwamoto, Y. Watanabe, T. Sadahiro, T. Haino and S. Yamago, *Angew. Chem. Int. Ed.*, 2011, **50**, 8342–8344.

11 Schrödinger, LLC, 2015.

12 J. W. Ochterski, .